expected consequence of Cu(II)-induced amide NH deprotonation, previously demonstrated by us to occur with apparent pK_a values of 3.1-3.2 in these cases.[13,15]

Rate data were also obtained (Table I) for the Cu(II)-catalyzed and uncatalyzed basic hydrolysis of two 8-hydroxyquinoline-based systems,[12] where spectral titrations indicated essentially complete saturation with 1 equiv of Cu(II). In these cases we did not generate pH-rate profiles, so that the "single-point" REF values listed must be taken as upper estimates. Even so, these REFs are seen to be smaller than that observed for (6-COOH)Pic-Sar, indicating that the 8-hydroxyquinoline ligand provides a Cu(II) of suboptimal catalytic power, probably on account of diminished Lewis acidity and/or a deleterious chelate geometry.

In summary, we have shown that structurally simple, coordinating amides containing *aliphatic* amine leaving groups are subject to marked Cu(II) catalysis[16] of the normal HO^--dependent hydrolysis when amide NH deprotonation is blocked; the apparent REFs are at least as large as the 10^5-10^7 REFs we saw previously for *aromatic* amine leaving groups (anilides) using Cu(II).[17] As in the anilide case, we cannot here distinguish between kinetically equivalent metal hydroxide (intramolecular) and carbonyl activation (with external HO^- attack) mechanisms. Nonetheless, the magnitude of catalysis reported in Table I is comparable to what Groves and co-workers observed for specially designed aliphatic lactams which control the stereoelectronics of metal ion-carbonyl interaction,[8] suggesting that such constraints are not absolute requirements for observing large catalytic effects. It thus appears that amide hydrolysis is *intrinsically* subject to metal ion catalysis to a degree which rivals that seen for ester hydrolysis, a notion which is not generally appreciated.

Acknowledgment. We thank Dr. P. K. Arora for help with ligand synthesis and the NIH (Grant GM-34294) for financial support. L.M.S. acknowledges a NIH Research Career Development Award (1987-1992).

Registry No. **1**, 125686-77-3; **2**, 5616-29-5; **3**, 125686-83-1; **4**, 125686-80-8; **5**, 138878-36-1; **6**, 125686-79-5; **7**, 138878-37-2; H-Sar-OCH_2Ph·TsOH, 54384-06-4; Pic-Sar-OCH_2Ph, 138878-38-3; Cu(N-$O_3)_2$, 3251-23-8; bis(pyridine-2,6-dicarboxylic acid)copper(II), 68398-38-9; 8-hydroxyquinoline-2-carboxylic acid, 1571-30-8.

Supplementary Material Available: A textual presentation of experimental details (2 pages). Ordering information is given on any current masthead page.

(15) (6-COOH)Pic-Gly-Cu(II) exhibits a coupled 2-proton dissociation with pK_a = 3.20 and a third dissociation with pK_a = 5.48, but amide dissociation occurs in the former instance. The latter pK_a probably corresponds to "outside" protonation of the carbonyl oxygen in the amide-*N*-ligated tridentate complex.

(16) Since complete hydrolysis can be achieved using substoichiometric amounts of Cu(II) (the rate slows down at proportional percent reactions due to the more favorable binding of Cu(II) to products than to reactants), we prefer to speak of metal ion *catalysis* rather than metal ion *promotion* of hydrolysis.

(17) Reddy, K. V.; Jacobson, A. R.; Kung, J. I.; Sayre, L. M. *Inorg. Chem.* **1991**, *30*, 3520.

Department of Chemistry
Case Western Reserve University
Cleveland, Ohio 44121

Lawrence M. Sayre*
K. Veera Reddy
Alan R. Jacobson
Wei Tang

Received September 6, 1991

EPR Studies of a Dinickel Complex in Its II,II and II,III Oxidation States

Bimetallic complexes of 2,6-bis[(bis(2-pyridylmethyl)amino)-methyl]-4-methylphenol (HMPMP) and related ligands have been found to exhibit a variety of interesting spectroscopic and magnetic properties.[1] The EPR spectra observed for these complexes have been useful in understanding the physical properties of diiron-oxo proteins in their diferrous and mixed-valence forms.[2] In turn, these complexes have in part allowed the development of a quantitative treatment of these signals.[3] The spectroscopic properties of model dinickel complexes are of interest[4] as models for the putative dinickel active site of jack bean urease.[5] In this communication, we report the detection of an integer-spin EPR signal from a $Ni^{II}Ni^{II}$ complex and the first observation of a half-integer-spin EPR signal from a mixed-valence $Ni^{II}Ni^{III}$ complex.

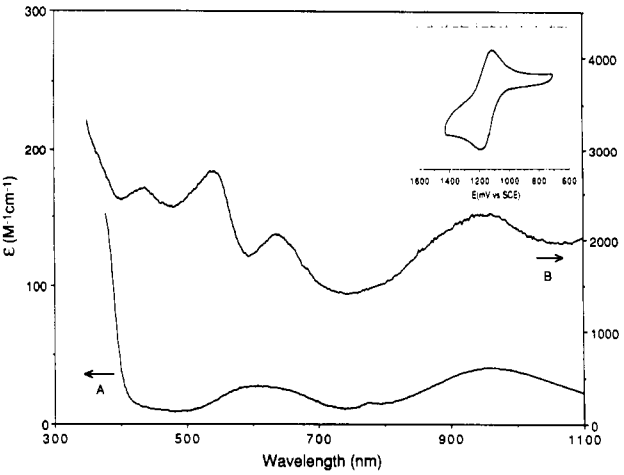

Figure 1. UV-vis absorption spectra of (A) **1** in CH_3CN at 23 °C and (B) **3** in CH_2Cl_2 at -50 °C. The cyclic voltammetry trace of **2** in CH_2Cl_2 is shown in the inset.

$[Ni_2BPMP(O_2CC_2H_5)_2]BPh_4·CH_3COCH_3$ (**1**) and $[Ni_2BPMP(O_2CCH_3)_2]ClO_4$ (**2**), obtained as pale blue crystals,[6] exhibit properties expected of complexes with (μ-phenoxo)bis(μ-carboxylato)dimetal cores such as $[Fe_2BPMP(O_2CC_2H_5)_2]BPh_4$.[1f]

(1) (a) Borovik, A. S.; Papaefthymiou, V.; Taylor, L. F.; Anderson, O. P.; Que, L., Jr. *J. Am. Chem. Soc.* **1989**, *111*, 6183-6195. (b) Suzuki, M.; Uehara, A.; Oshio, H.; Endo, K.; Yanaga, M.; Kida, S.; Saito, K. *Bull. Chem. Soc. Jpn.* **1987**, *60*, 3547-3555. (c) Mashuta, M. S.; Webb, R. J.; Oberhausen, K. J.; Richardson, J. F.; Buchanan, R. M.; Hendrickson, D. N. *J. Am. Chem. Soc.* **1989**, *111*, 2745-2746. (d) Holman, T. R.; Andersen, K. A.; Anderson, O. P.; Hendrich, M.; Juarez-Garcia, C.; Münck, E.; Que, L., Jr. *Angew. Chem., Int. Ed. Engl.* **1990**, *29*, 921-923. (e) Holman, T. R.; Juarez-Garcia, C.; Hendrich, M. P.; Que, L., Jr.; Munck, E. *J. Am. Chem. Soc.* **1990**, *112*, 7611-7618. (f) Borovik, A. S.; Hendrich, M. P.; Holman, T. R.; Munck, E.; Papaefthymiou, V.; Que, L., Jr. *J. Am. Chem. Soc.* **1990**, *112*, 6031-6038.

(2) (a) Hendrich, M. P.; Münck, E.; Fox, B. G.; Lipscomb, J. D. *J. Am. Chem. Soc.* **1990**, *112*, 5861-5865. (b) Day, E. P.; David, S. S.; Peterson, J.; Dunham, W. R.; Bonvoisin, J. J.; Sands, R. H.; Que, L., Jr. *J. Biol. Chem.* **1988**, *263*, 15561-15567. (c) Reem, R. C.; Solomon, E. I. *J. Am. Chem. Soc.* **1987**, *109*, 1216-1226. (d) Hendrich, M. P.; Pearce, L. L.; Que, L., Jr.; Chasteen, N. D.; Day, E. P. *J. Am. Chem. Soc.* **1991**, *113*, 3039-3044.

(3) Juarez-Garcia, C.; Hendrich, M. P.; Holman, T. R.; Que, L., Jr.; Munck, E. *J. Am. Chem. Soc.* **1991**, *113*, 518-525.

(4) (a) Buchanan, R. M.; Mashuta, M. S.; Oberhausen, K. J.; Richardson, J. F.; Li, Q.; Hendrickson, D. N. *J. Am. Chem. Soc.* **1989**, *111*, 4497-4498. (b) Chaudhuri, P.; Kuppers, H.-J.; Wieghardt, K.; Gehring, S.; Haase, W.; Nuber, B.; Weiss, J. *J. Chem. Soc. Dalton Trans.* **1988**, 1367-1370. (c) Turpeinen, U.; Hämäläinen, R.; Reedijk, J. *Polyhedron* **1987**, *6*, 1603-1610. (d) Ahlgren, M.; Turpeinen, U.; Hamalainen, R. *Acta Chem. Scand.* **1978**, *A32*, 189-194. (e) Ahlgren, M.; Turpeinen, U. *Acta Crystallogr.* **1982**, *B38*, 1580-1583. (f) Rojo, T.; Cortes, R.; Lezama, L.; Mesa, J. L.; Villeneuve, G. *Inorg. Chim. Acta* **1989**, *162*, 11-13.

(5) (a) Dixon, N. E.; Gazzola, C.; Blakeley, R. L.; Zerner, B. *J. Am. Chem. Soc.* **1975**, *97*, 4131-4133. (b) Clark, P. A.; Wilcox, D. E. *Inorg. Chem.* **1989**, *28*, 1326-1333. (c) Clark, P. A.; Wilcox, D. E.; Scott, R. A. *Inorg. Chem.* **1990**, *29*, 579-581.

(6) Complex **1** was synthesized similarly to the $[Fe_2BPMP(\mu$-$O_2CC_2H_5)_2](BPh_4)_2$ complex. Anal. Calcd for $C_{66}H_{69}BN_6Ni_2O_6$: C, 67.72; H, 5.94; N, 7.18; Ni, 10.02. Found: C, 67.46; H, 6.08; N, 7.43; Ni, 9.68. The preparation of compound **2** involved the sequential addition of 2 equiv of $Ni(OAc)_2·4H_2O$ and 2 equiv of NEt_4ClO_4 to a methanolic solution of HBPMP. The resulting mixture slowly evaporated at 10 °C, yielding crystals (≈64%) which were spectroscopically identical to **1**. Anal. Calcd for $C_{37}H_{39}N_6ClNi_2O_9$: C, 51.40; H, 4.55; N, 9.72. Found: C, 51.35; H, 4.69; N, 9.48.

0020-1669/92/1331-0937$03.00/0 © 1992 American Chemical Society

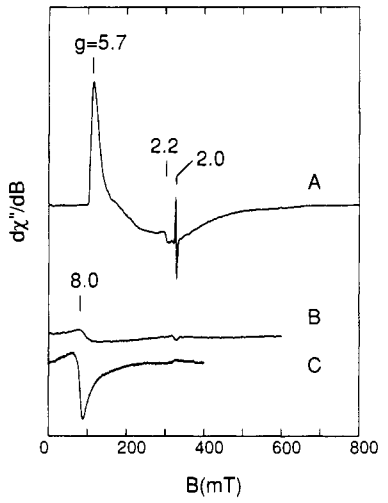

Figure 2. X-Band (9.1 GHz, 0.2 mW) EPR spectra of (A) **3** at $T = 3$ K and (B, C) **1** at $T = 20$ K, both 1 mM in CH_2Cl_2. The spectra are on the same instrumental vertical scale except trace A has been reduced by a factor of 10. Traces A and B are recorded with the microwave magnetic field transverse to the static field, whereas for trace C these fields are parallel.

The IR spectrum of **1** (KBr pellet) displays strong absorptions at 1602 and 1427 cm^{-1} which correspond to the ν_s and ν_{as} bands, respectively, of bridging carboxylates and are typical of similar complexes.[1e,1f,7] The electronic absorption spectrum for complex **1** in acetonitrile suggests an octahedral environment for the two Ni(II) ions (Figure 1A). Two broad absorption bands are observed at 602 nm ($\epsilon = 27$ M^{-1} cm^{-1}) and 962 nm ($\epsilon = 35$ M^{-1} cm^{-1}), which can be assigned to the $^3A_{2g} \rightarrow {}^3T_{1g}(F)$ and $\rightarrow {}^3T_{2g}(F)$ transitions, respectively. A weak band is also observed at 780 nm ($\epsilon \approx 6$ M^{-1} cm^{-1}), which is ascribed to the spin-forbidden transition $^3A_{2g} \rightarrow {}^1E_{1g}$. Another spin-allowed d–d transition, normally observed for octahedral Ni(II) complexes between 350 and 420 nm,[8] is obscured by a strong absorption at 318 nm ($\epsilon = 4000$ M^{-1} cm^{-1}), which may arise from a transition involving Ni(II) and pyridine orbitals.[9] The ligand field bands observed can be related to the Tanabe–Sugano diagram for an octahedral d^8 system, resulting in the following crystal field parameters: $D_q = 1040$ cm^{-1} and $B \approx 860$ cm^{-1}.[10] These results compare well with those for two other bimetallic octahedral Ni(II) complexes with similar triply bridged cores.[4a,b]

Complex **1** displays a low-field EPR spectrum with a feature near $g = 8$ (Figure 2B). For a microwave magnetic field aligned parallel to the static field (Figure 2C), the resonance is sharper and more intense. These spectral changes indicate that the metal center giving rise to the resonance has an even number of unpaired electrons (integer spin).[11] The position of the resonance suggests that it originates from a doublet within a $S = 2$ spin manifold. The signal intensity at 3 K is weak but grows markedly as the temperature is increased, indicating that the signal is from an excited spin doublet. Under the assumption that the signal originates from the $S = 2$ quintet of a spin-coupled Ni(II) pair ($S_1 = S_2 = 1$) with negligible zero-field splittings (D_1, D_2) for the individual Ni sites, the temperature dependence of the signal gives $J = -1$ cm^{-1} ($H_{ex} = -2JS_1 \cdot S_2$).

The temperature dependence of the solid-state magnetic susceptibility for complex **1** suggests a weakly antiferromagnetically coupled dinickel unit, as seen by the gradual decrease of the χT value from 2.4 to 1.4 cm^3 mol^{-1} K upon cooling the sample from ambient to liquid-helium temperatures. The theoretical powder average curve was calculated from the spin Hamiltonian as described previously,[12] and the parameters obtained were $J = -1.2$ (2) cm^{-1}, $g_{Ni} = 2.19$ (4), and negligible D_1 and D_2 values, in agreement with the EPR data. No satisfactory fit to both the EPR and magnetization data was found for $J < D_1, D_2$. The exchange coupling observed and the negligible zero-field splittings are consistent with the results on $[Ni_2bimp(OAc)_2]ClO_4$ (Hbimp = 2,6-bis[(bis((1-methyl-2-imidazolyl)methyl)amino)methyl]-4-methylphenol).[4a]

Cyclic voltammetry on complex **2** in CH_2Cl_2, with tetrabutylammonium tetrafluoroborate as the electrolyte, reveals a reversible one-electron redox wave at +1.135 V vs SCE ($E(Fc^+/Fc) = 0.550$ V), assigned to the $Ni^{III}Ni^{II}/Ni^{II}Ni^{II}$ couple (see insert, Figure 1). This couple is more anodic than those for two other $Ni^{II}Ni^{II}$ complexes: $[Ni_2bimp(OAc)_2]^+$ (0.94 V vs Ag/AgCl)[4a] and $[Ni_2(OH)(OAc)_2(Me_3TACN)_2]^+$ (0.38 V vs Fc/Fc^+; Me_3TACN = 1,4,7-trimethyl-1,4,7-triazacyclononane).[4b] The $Ni^{II}Ni^{III}$ complex (**3**) can be generated in CH_2Cl_2 by bulk electrolysis at low temperature (−50 °C) with rigorous exclusion of water. Upon one-electron oxidation of the $Ni^{II}Ni^{II}$ complex (as measured by coulometry), the pale blue solution acquires a dark brown purple color. This transformation is reversible, and the complex can be reoxidized after reduction to the Ni^{II}_2 form.[13] The UV–vis spectrum of **3** (Figure 1B) shows a complex series of absorption features at 432 nm ($\epsilon \approx 2600$ M^{-1} cm^{-1}), 542 nm ($\epsilon \approx 2800$ M^{-1} cm^{-1}), 636 nm ($\epsilon \approx 1900$ M^{-1} cm^{-1}), and 968 nm ($\epsilon \approx 2300$ M^{-1} cm^{-1}).[14] Similar features are observed for $[Ni^{III}TAAB]^+$ (TAAB = tetrabenzo[*b,f,j,n*][1,5,9,13]tetraazacyclohexadecane),[15] but the nature of these transitions has not been assigned.

At 2.2 K, complex **3** exhibits an EPR signal with a relatively sharp feature at $g = 5.7$ and a broad feature centered around $g = 2.0$[16] (Figure 2A); the signal increases in intensity as the temperature is lowered, indicating that it originates at least in part from a ground spin doublet.[17] This signal is similar to that observed for the complex $[Fe^{III}Ni^{II}BPMP(O_2CC_2H_5)_2](BPh_4)_2$, where the metals are antiferromagnetically coupled ($S_{Fe} = {}^5/_2$, $S_{Ni} = 1$) to give a ground $S = {}^3/_2$ manifold.[1e] Accordingly, the spectrum of **3** is also assigned to a rhombic $S = {}^3/_2$ system; however, in this case the signal most likely originates from a ferromagnetically coupled pair consisting of high-spin Ni(II) ($S_1 = 1$) and low-spin Ni(III) ($S_2 = {}^1/_2$). Other coupling formulations have been ruled out for the following reasons. A high-spin Ni(III) ($S = {}^3/_2$) coupled to a high-spin Ni(II) ($S = 1$) would yield either an $S = {}^1/_2$ (antiferromagnetic) or an $S = {}^5/_2$ (ferromagnetic)

(7) (a) Nakamoto, K. *Infrared and Raman Spectra of Inorganic and Coordination Compounds*, 3rd ed.; Wiley: New York, 1978; p 232. (b) Mehrotra, R. C.; Bohra, R. *Metal Carboxylates*; Academic Press: New York, 1983; p 53.
(8) (a) Whyman, R.; Hatfield, W. E.; Paschal, J. S. *Inorg. Chim. Acta* **1967**, *1*, 113–119. (b) Nathan, L. C.; Nelson, J. H.; Rich, G. L.; Ragsdale, R. O. *Inorg. Chem.* **1969**, *8*, 1494–1497. (c) Ball, P. W.; Blake, A. B. *J. Chem. Soc. A* **1969**, 1415–1422. (d) Duggan, D. M.; Hendrickson, D. N. *Inorg. Chem.* **1974**, *13*, 2056–2062.
(9) Barefield et al. has reported the UV–vis spectrum of the $[Ni^{II}CR]^{2+}$ complex (CR = 2,12-dimethyl-1,7,11,17-tetraazabicyclo[11.3.1]heptadeca-1(17),2,11,13,15-pentaene). In this ligand, a pyridine is incorporated into the cyclam ring. The complex displays strong CT bands at 390 nm (ϵ 1450) and 310 nm (ϵ 3380). This indicates that the large CT band in **2** may also originate from the pyridine ligands: Barefield, E. K.; Lovecchio, F. V.; Tokel, N. E.; Ochiai, E.; Busch, D. H. *Inorg. Chem.* **1972**, *11*, 283–288.
(10) Figgis, B. N. *Introduction to Ligand Fields*; Interscience: New York, 1966.
(11) Hendrich, M. P.; Debrunner, P. G. *Biophys. J.* **1989**, *56*, 489–506.
(12) Day, E. P.; Kent, T. A.; Lindahl, P. A.; Münck, E.; Orme-Johnson, W. H.; Roder, H.; Roy, A. *Biophys. J.* **1987**, *52*, 837–853.
(13) The $Ni^{II}Ni^{III}$ complex is unstable at room temperature; however, it is stable in solution at −50 °C for upward of 3 h, as demonstrated by its UV–vis absorption spectrum.
(14) The apparatus used to record the −50 °C spectrum consisted of a jacketed, vacuum-sealed quartz sample holder which contained cooled methanol. The quality of the near-IR data was consistently bad due to the strong absorption from the cooling solvent which inhibited reliable baseline subtraction.
(15) Takvoryan, N.; Farmery, K.; Katovic, V.; Lovecchio, F. V.; Gore, E. S.; Anderson, L. B.; Busch, D. H. *J. Am. Chem. Soc.* **1974**, *96*, 731–742.
(16) The feature at $g = 2.2$ is present in several preparations with the same intensity; however, simulations of the $g = 5.7$ signal suggest that the $g = 2.2$ feature is not associated with the same spin system. The sharp feature at $g = 2$ is from an impurity radical species.
(17) In a rhombic $S = {}^3/_2$ system, both doublets can give rise to features in the $g = 5.5$ region, making it difficult to determine their relative contributions to the spectrum.

ground state; the $S = {}^3/_2$ state would be an excited state in contradiction with the ground-state assignment of the above signal. An $S = {}^3/_2$ signal could conceivably arise from a high-spin Ni(III) ($S = {}^3/_2$) with weak or vanishing coupling to an EPR-silent Ni(II) ($S = 1$); however, this appears unlikely, given that all known Ni(III) complexes to date are low spin[18] and that in all complexes of BPMP involving two paramagnetic metal ions thus far some degree of coupling is observed.[1a,b,d-f]

The observed ferromagnetic coupling may be rationalized by an examination of the magnetic orbitals of the two nickel centers under the assumption that the phenolate bridge dominates the coupling interaction of the complex, an assumption supported by our studies of FeCuBPMP complexes.[1d,e] Jahn-Teller elongation of the low-spin Ni(III) (d^7) site along an axis orthogonal to the phenolate bond[19,20] would place the magnetic orbital (d_{z^2})[21] parallel to the elongation axis and orthogonal to the phenolate bond, engendering ferromagnetic coupling. A Jahn-Teller elongation has previously been observed in the crystal structure of $[Fe^{III}Cu^{II}BPMP(O_2CCH_3)_2](BPh_4)_2$,[1d] in which case, the magnetic orbital ($d_{x^2-y^2}$) is directed along the phenolate bond and antiferromagnetic coupling is observed. It is not unreasonable to propose similar structural properties in the $Ni^{III}Ni^{II}$ complex, which would explain the observed spectroscopic result.

In conclusion, we have reported the unambiguous observation of an integer-spin EPR signal from an antiferromagnetically coupled $Ni^{II}Ni^{II}$ cluster. The existence of such a signal may help in the further investigations of similar centers in model inorganic complexes as well as in the active site of urease. In addition, we have generated and characterized some properties of the first $Ni^{III}Ni^{II}$ mixed-valence complex.

Acknowledgment. We are grateful to Prof. J. D. Lipscomb for use of his EPR spectrometer. This work was supported by National Institutes of Health Grant GM38767 (L.Q.), Postdoctoral Fellowship GM12996 (M.P.H.), and Predoctoral Traineeship GM08277 (T.R.H.).

(18) (a) Lappin, A. G.; Murray, C. K.; Margerum, D. W. *Inorg. Chem.* **1978**, *17*, 1630-1634. (b) Haines, R. I.; McAuley, A. *Coord. Chem. Rev.* **1981**, *39*, 77-119. (c) Salerno, J. C. In *The Bioinorganic Chemistry of Nickel*; Lancaster, J. R., Ed.; VCH: New York, 1988; pp 53-72.
(19) Lovecchio, F. V.; Gore, E. S.; Busch, D. H. *J. Am. Chem. Soc.* **1974**, *96*, 3109-3118.
(20) de Castro, B.; Freire, C. *Inorg. Chem.* **1990**, *29*, 5113-5119.
(21) The EPR spectra of low-spin Ni(III) complexes associate the magnetic orbital with the d_{z^2} orbital.[18]

Department of Chemistry
University of Minnesota
Minneapolis, Minnesota 55455

Theodore R. Holman
Michael P. Hendrich
Lawrence Que, Jr.*

Received July 26, 1991

Characterization of Fe(OEP) π-Cation Radicals

We report the characterization of two classes of π-cation-radical derivatives of (octaethylporphinato)iron(III): $[Fe(OEP^{\bullet})(OClO_3)_2]$,[1] and $[Fe(OEP^{\bullet})(Cl)]Y$, where $Y = ClO_4^-$ or $SbCl_6^-$. A combination of crystal structure determination, magnetic susceptibility measurement, and Mössbauer spectroscopy leads to an unambiguous assignment of the iron spin states and gives insight into the nature of the porphyrin radical/iron spin coupling. Our conclusions are distinctly different from those recently reported by Nakashima et al.,[2,3] which were based solely on magnetic susceptibility results.

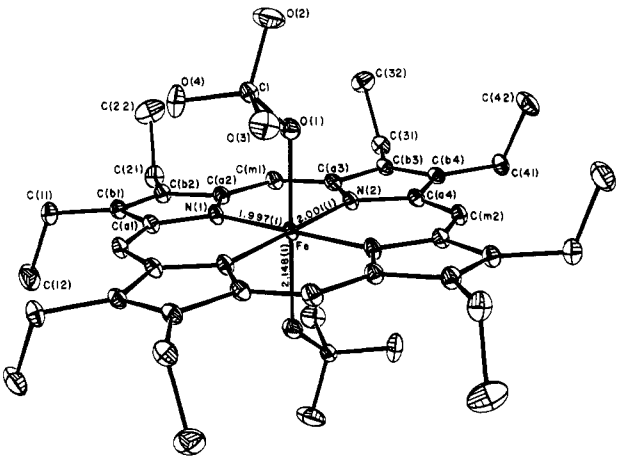

Figure 1. ORTEP diagram of the molecular structure of the $[Fe(OEP^{\bullet})(OClO_3)_2]$ complex. Thermal ellipsoids are drawn at the 50% probability level. Hydrogen atoms omitted for clarity.

Six-coordinate $[Fe(OEP^{\bullet})(OClO_3)_2]$ was prepared by oxidation of $[Fe(OEP)(OClO_3)]$ with thianthrenium perchlorate.[4-8] The single-crystal sample, prepared from [Fe(OEP)Cl], has a minor chloride impurity; bulk samples are homogeneous by Mössbauer criteria. The molecular structure of $[Fe(OEP^{\bullet})(OClO_3)_2]$ is illustrated in Figure 1.[9] The monomeric complex has two axial perchlorate ligands with an in-plane iron atom located at an inversion center. The average value of the Fe-N_p bond distances is 1.999 (2) Å, which is inconsistent with a high-spin state for iron.[11] The analogous $TTP^{\bullet}$ complex[6] has an average Fe-N_p bond distance of 2.068 (21) Å, consistent with the assigned high-spin state. The porphinato core is planar, consistent with the required inversion symmetry. Both this molecular structure and the diagnostically large quadrupole splitting in the zero-field Mössbauer spectrum ($\Delta E_q = 3.00$ mm/s and $\delta = 0.43$ mm/s, 4.2 K) show that the iron(III) atom has an *admixed intermediate-spin* state, rather than the high-spin state assumed by others[2] and seen for the analogous $TPP^{\bullet}$ and $TTP^{\bullet}$ derivatives.[6,12] The intermedi-

(1) Abbreviations: OEP, TPP, and TTP, dianions of octaethyl-, tetraphenyl-, and tetratolylporphyrin, respectively; π-cation-radical derivatives are indicated with a raised dot in the formula (i.e., $OEP^{\bullet}$).

(2) Nakashima, S.; Ohya-Nishiguchi, H.; Hirota, N.; Fujii, H.; Morishima, I. *Inorg. Chem.* **1990**, *29*, 5207.
(3) Our high-temperature magnetic moments for $[Fe(OEP^{\bullet})(OClO_3)_2]$ are significantly lower than those of Nakashima et al. Although our magnetic susceptibility data for $[Fe(OEP^{\bullet})(Cl)][SbCl_6]$ are quite similar to those of Nakashima et al., we are unable to achieve satisfactory fits with their parameters.
(4) Gans, P.; Marchon, J.-C.; Reed, C. A.; Regnard, J.-R. *Nouv. J. Chim.* **1981**, *5*, 203.
(5) Murata, Y.; Shine, H. J. *J. Org. Chem.* **1969**, *34*, 3368.
(6) Gans, P.; Buisson, G.; Duée, E.; Marchon, J.-C.; Erler, B. S.; Scholz, W. F.; Reed, C. A. *J. Am. Chem. Soc.* **1986**, *108*, 1223.
(7) Shimomura, E. T.; Phillippi, M. A.; Goff, H. M.; Scholz, W. F.; Reed, C. A. *J. Am. Chem. Soc.* **1981**, *103*, 6778. Phillippi, M. A.; Goff, H. M. *J. Am. Chem. Soc.* **1982**, *104*, 6778.
(8) Synthetic details for single crystals and bulk samples of $[Fe(OEP^{\bullet})(OClO_3)_2]$ are given in the supplementary material. UV-vis (CH_2Cl_2 solution): λ_{max} 378 (Soret), 480 nm. IR (KBr) $\nu(OEP^{\bullet})$ 1531 cm^{-1} (broad); $\nu(ClO_4)$ 1145 (strong), 1108 (strong, broad), 636, 627 cm^{-1}.
(9) $[Fe(OEP^{\bullet})(OClO_3)_2]$ crystallizes in the triclinic space group $P\bar{1}$, a = 9.530 (3) Å, b = 9.580 (2) Å, c = 10.756 (2) Å, α = 88.96 (2)°, β = 77.06 (2)°, γ = 68.72 (2)°, V = 889.7 Å^3, and $Z = 1$. A total of 8092 reflections were measured (6082 unique) at 123 K and 5184 reflections having $(\sin\theta)/\lambda < 0.742$ and $F_o \geq 3.0\sigma(F_o)$ were taken as observed. The structure was solved using the program DIRDIF[10] and difference Fouriers. A small amount of an impurity (<7% of [Fe(OEP)(Cl)]) was included in the final model. Unlike the bulk samples, single crystals were derived from [Fe(OEP)(Cl)] rather than $[Fe(OEP)(OClO_3)]$. Least-squares refinement of the model based on 298 variables with anisotropic thermal parameters for all major occupancy non-hydrogen atoms and fixed, idealized hydrogen atoms leads to $R_1 = 0.041$, $R_2 = 0.054$, and goodness of fit = 1.91.
(10) Beurskens, P. T.; Bosman, W. P.; Doesbury, H. M.; Gould, R. O.; van den Hark, Th. E. M.; Prick, P. A.; Noordik, J. H.; Stempel, M.; Smits, J. M. M. *DIRDIF*; Technical Report 1984/1; Crystallography Laboratory: Toernooiveld, 6525 Ed Nijmegen, The Netherlands.
(11) Scheidt, W. R.; Reed, C. A. *Chem. Rev.* **1981**, *81*, 543.

0020-1669/92/1331-0939$03.00/0 © 1992 American Chemical Society